UniMi, IASF-BO, UniTs, OATs, UCSB

LFI Project System Team

Planck LFI

Prepared by	A. Mennella, L. Terenzi, A. Zonca, G. Morgante, F. Cuttaia, A. Gregorio	May 30, 2010
Agreed by	M. Bersanelli LFI Instrument Scientist C.R. Butler LFI Program Manager	May 30, 2010
Approved by	N. Mandolesi LFI Principal Investigator	May 30, 2010

CHANGE RECORD

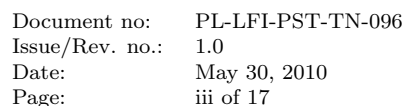| Issue	Date	Sheet	Description of change	Release
0.1	18th May, 2010	All	First draft of document	0.1
0.2	25th May, 2010	All	Second draft of document	0.2
1.0	30th May, 2010	All	First Issue of document	1.0

DISTRIBUTION LIST

Recipient	Company/Institute	E-mail address	Sent
J. Tauber	ESA/PSO	jtauber@rssd.esa.int	Yes
C. Watson	ESA/ESOC	Christopher.J.Watson@esa.int	Yes
N. Mandolesi	INAF/IASFBO	reno@iasfbo.inaf.it	Yes
M. Bersanelli	UniMi	marco.bersanelli@fisica.unimi.it	Yes
C. Butler	INAF/IASFBO	butler@iasfbo.inaf.it	Yes
A. Zacchei	INAF/OATs	zacchei@oats.inaf.it	Yes
A. Mennella	UniMi	aniello.mennella@fisica.unimi.it	Yes
A. Gregorio	UniTs	anna.gregorio@ts.infn.it	Yes
L. Terenzi	INAF/IASFBO	terenzi@iasfbo.inaf.it	Yes
G. Morgante	INAF/IASFBO	morgante@iasfbo.inaf.it	Yes
F. Cuttaia	INAF/IASFBO	cuttaia@iasfbo.inaf.it	Yes
A. Zonca	UCSB	zonca@deepspace.ucsb.edu	Yes
PSO		pso_operations@sciops.esa.in	Yes
Cryogenic Working Group		coeg@rssd.esa.int	Yes
HFI operation team		lfi-operations@oats.inaf.it	Yes
LFI operation team		hfi-operations@ias.u-psud.fr	Yes
LFI systematics		lfi_systematics@iasfbo.inaf.it	Yes

	Impact of Sorption-Cooler induced temperature fluctuations on Planck-LFI: evaluation using data measured in flight.	Document no:	PL-LFI-PST-TN-096
		Issue/Rev. no.:	1.0
		Date:	May 30, 2010
		Page:	iv of 17

Contents

Abstract

In this technical note we present an evaluation of the effect of sorption cooler induced temperature fluctuations Planck-LFI using temperature data measured in flight. In particular we analyse three scenarios in order to evaluate the effect of TSA capability to damp temperature fluctuations at the sorption cooler cold end. The first scenario is one in which the TSA is completely off and the LFI is subject to the complete spectrum of the cold end temperature variations. The second scenario is one in which the TSA is working nominally and the third scenario is one in which the TSA is working in a not-nominal situation because of sorption-cooler aging. The analysis, performed with two, independent methods, show clearly a negative impact of the increased level of temperature fluctuations on the LFI maps. In particular, estimates of the effect in case the TSA were kept off for a significant fraction of the sky coverage indicate that the effect would not be compatible with the LFI scientific requirements.

1 Applicable and Reference Documents

Reference Documents

[RD1] A. Mennella et al. Effect of Sorption Cooler Temperature Variations on the LFI Front–End. Technical Report PL-LFI-PST-TN-005 2.0, IFC–CNR, October 2001.

[RD2] A. Mennella. Impact of Sorption Cooler induced temperature fluctuations on PLANCK–LFI maps: first–order evaluation using EBB data. IASF–CNR Sez. di Milano, June 2002.

[RD3] A. Mennella. Impact of Sorption Cooler induced temperature fluctuations on PLANCK–LFI maps: first–order evaluation using EBB data with PID control. IASF–CNR Sez. di Milano, April 2003.

[RD4] A. Mennella. Impact of Sorption Cooler induced temperature fluctuations on PLANCK–LFI maps: first–order evaluation using EBB data with PID control. IASF–CNR Sez. di Milano, April 2003.

[RD5] A. Mennella. Impact of Sorption Cooler induced temperature fluctuations on PLANCK–LFI: evaluation using data measured at JPL during May-June 2004 with PID control. IASF–CNR Sez. di Milano, June 2004.

[RD6] A. Mennella, M. Bersanelli, C. Burigana, D. Maino, N. Mandolesi, G. Morgante, and G. Stanghellini. PLANCK: Systematic effects induced by periodic fluctuations of arbitrary shape. *A&A*, 384:736–742, 2002.

[RD7] A. Mennella, M. Seiffert, and M. Bersanelli. Temperature stability requirements of the LFI Sorption Cooler cold-end (LR2). Technical report, IASF-MI–CNR, September 2002.

[RD8] M. Seiffert, A. Mennella, C. Burigana, N. Mandolesi, M. Bersanelli, P. Meinhold, and P. Lubin. 1/f noise and other systematic effects in the Planck-LFI radiometers. *A&A*, 391:1185–1197, September 2002.

[RD9] L. Terenzi and LFI calibration team. Planck LFI CPV: Thermal Susceptibility Test Report (ref: P_PVP_LFI_0016_01)). Technical Report PL-LFI-PST-RP-075 1.1, UniMi, UniTs, INAF/OATs, IASF-BO, UCSB, ESA, Univ. Helsinki, Oct 2009.

[RD10] L. Terenzi and LFI calibration team. Planck LFI CPV: TSA Failure and Thermal Dynamic Response (ref: P_PVP_LFI_0023_01). Technical Report PL-LFI-PST-RP-078 1.1, UniMi, UniTs, INAF/OATs, IASF-BO, UCSB, ESA, Univ. Helsinki, Oct 2009.

UniMi, IASF-BO, UniTs, OATs, UCSB
LFI Project System Team

Impact of Sorption-Cooler induced temperature fluctuations on Planck-LFI: evaluation using data measured in flight.

Document no: PL-LFI-PST-TN-096
Issue/Rev. no.:   1.0
Date: May 30, 2010
Page: 2 of 17

[RD11] L. Terenzi, M.J. Salmon, A. Colin, A. Mennella, G. Morgante, M. Tomasi, P. Battaglia, M. Lapolla, M. Bersanelli, R.C. Butler, F. Cuttaia, O. D'Arcangelo, R. Davis, C. Franceschet, S. Galeotta, A. Gregorio, N. Hughes, P. Jukkala, D. Kettle, M. Laaninen, P. Leutenegger, R. Leonardi, N. Mandolesi, M. Maris, P. Meinhold, M. Miccolis, N. Roddis, L. Sambo, M. Sandri, R. Silvestri, L. Valenziano, J. Varis, F. Villa, A. Wilkinson, and A. Zonca. Thermal susceptibility of the Planck-LFI receivers. *JINST*, 4:T12012, dec 2009.

[RD12] M. Tomasi, G. Baldan, M. Lapolla, A. Mennella, G. Morgante, L. Pagan, and L. Terenzi. Thermal models of the Planck/LFI QM/FM instruments. In *Modeling, Systems Engineering, and Project Management for Astronomy II. Edited by Cullum, Martin J.; Angeli, George Z.. Proceedings of the SPIE, Volume 6271, pp. 62710X (2006).*, volume 6271 of *Presented at the Society of Photo-Optical Instrumentation Engineers (SPIE) Conference*, July 2006.

[RD13] M. Tomasi, B. Cappellini, A. Gregorio, F. Colombo, M. Lapolla, L. Terenzi, G. Morgante, M. Bersanelli, R. C. Butler, S. Galeotta, N. Mandolesi, M. Maris, A. Mennella, L. Valenziano, and A. Zacchei. Dynamic validation of the Planck-LFI thermal model. *JINST*, 5:T01002, jan 2010.

Applicable Documents

[AD1] M. Bersanelli, A. Mennella, M. Seiffert, and R. Hoyland. PLANCK–LFI Scientific Requirements. Technical Report PL-LFI-PST-SP-011 2.0, IASF–UNIMI, March 2002.

2   Introduction

A high degree of temperature stability of the Planck-LFI 20 K unit hosting the front-end part of the pseudo correlation receivers is of key importance in the LFI systematic error control strategy. In fact, any temperature fluctuation at the level of the interface between the cooler LR2 cold end and the instrument propagates through the mechanical structure and couples with the radiometric measurements leaving an imprint on the final maps and power spectra.

The importance of this effect was recognised very early in the LFI programme and since year 2000 a considerable amount of work has been dedicated to understand the impact of temperature fluctuations on the measured radiometric signal (see, for example, [RD1, RD7, RD3, RD2, RD4, RD5]).

A temperature stabilisation assembly (TSA) has been developed by the Sorption Cooler team in order to control the level of temperature fluctuations at the Sorption Cooler cold end and damp, in particular, the low frequency fluctuations, which are the ones that are not effectively damped by the instrument mechanical structure.

The TSA is based on a resistance that provides a small variable heating power at the cold end interface; the heating power variations are controlled by a PID (Proportional, Integral, Derivative) circuit which compensates the cold-end temperature fluctuations and maintain the interface temperature as close as possible to a temperature value (named *setpoint*) which is slightly higher than the cold-end temperature.

As the cooler ages the level of temperature fluctuations increases, the cooling power decreases and the TSA effectiveness decreases as well. After about 9 months of operations we have had evidence of such process and the Sorption Cooler team responded by a series of increase steps in the TSA setpoint in order to compensate for the increase in the temperature fluctuation level.

In this note we have attempted a preliminary evaluation of the impact of Sorption Cooler temperature fluctuations on the LFI science in order to estimate the impact of the TSA on the scientific products quality. We have first performed an analysis using a simple analytical model that allows to estimate the peak-to-peak final systematic effect on a map starting from a fluctuation of general shape, then we have build simulated maps using housekeeping sensor data filtered with radiometric transfer functions to approximate the expected spurious effect in the radiometric timeline.

In Section 4 we summarise the various procedures used to obtain the scientific impact estimates, while in Section 5 we outline and discuss results obtained with both methods. Main conclusions are summarised in Section 6.

3   Summary of measured temperature fluctuations in flight

In this section we report the details of the temperature data used for the analysis. We have used three sections of data relative to the temperature sensor SM020540 placed at the interface between the TSA and the LFI (sampling time 1 minute) - see Figure 1. The considered time sections have been the following:

- from 2009-07-29T06:22:17Z to 2009-07-29T09:58:25Z during the TSA failure text performed during CPV [RD10];

- from 2009-12-01T04:00:00Z to 2009-12-01T11:59:59Z during nominal operations (nominal temperature fluctuations);

- from 2010-05-11T04:00:01Z to 2010-05-11T11:59:59Z during nominal operations (increased level of temperature fluctuations).

4   Estimate of effect on maps

4.1   Scientific requirements

In the LFI scientific requirement document [AD1] a detailed budget of systematic errors has been provided. In the Table 3 we report the breakdown of these requirements for what concerns periodic thermal systematic effects in terms of error per physical pixel; the first row, in particular, is relative to thermal fluctuations of the front end of the LFI instrument. The global requirement on the maximum systematic effect from front-end temperature fluctuations is obtained by summing in quadrature the two terms in the first row (relative to spin-synchronous and periodic fluctuations) and is of the order of $\sim \pm 1\mu K$ ($\sim 2\mu K$ peak-to-peak).

In the following section we report the evaluation of the effect of temperature fluctuations on the LFI maps for the various datasets. The assessment has been peformed using the analytical method described in detail in [RD6].

4.2   Propagation of the systematic effect from the Sorption Cooler cold end to the map

Thermal damping curves   Thermal fluctuations at the interface between the LVHX2 cold end and the LFI focal plane propagate through the mechanical structure of the instrument and are
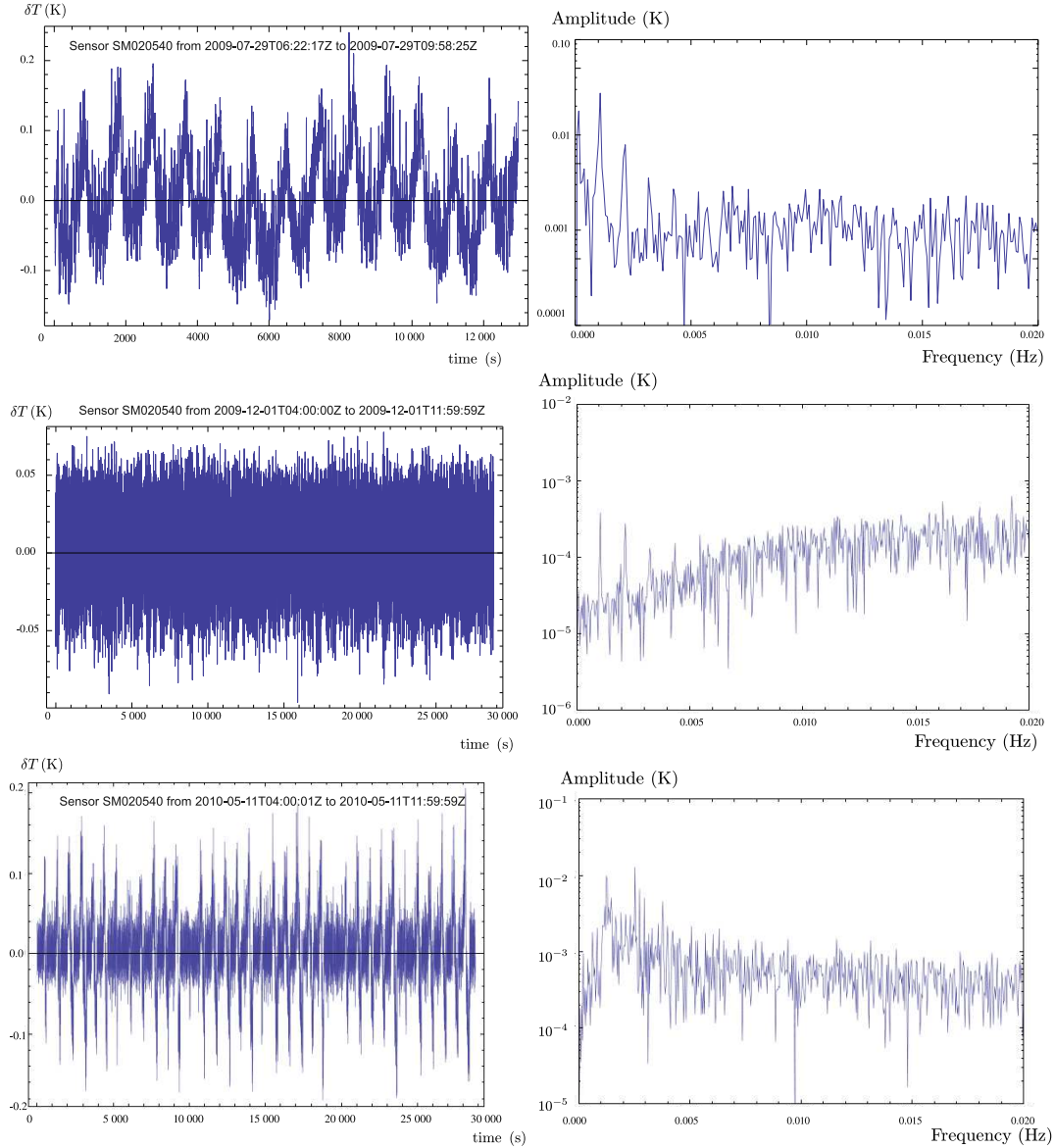
Figure 1: Timestream and frequency spectrum of temperature fluctuations measured on the TSA interface. Top: during TSA failure CPV test; middle: during nominal operations with nominal temperature fluctuations; bottom: during nominal operations with increased temperature fluctuations.

damped in amplitude and shifted in phase when reaching the instrument FEMs. Then, starting from the measurement of cold end temperature curves, the actual thermal fluctuations at the receivers can be evaluated knowing the thermal damping curves. These have been calculated using the LFI thermal model which is described in [RD13, RD12]. The thermal model was verified correlating the focal plane temperature sensor measured curves with the modelled ones. Once

Table 3: Breakdown of LFI thermal systematic effect requirements. The requirement for systematic effects induced by front-end temperature fluctuations is of the order of ~ 2 μK/pixel peak-to-peak (obtained by summing in quadrature the error from spin-syncronous and from other periodic fluctuations).

Source	Error from spin synch oscillations	Error from other periodic oscillations
Front End	± 0.45 μK	± 0.90 μK
WGs	± 0.40 μK	± 0.40 μK
BEMs	± 0.40 μK	± 0.40 μK
DAE	± 0.40 μK	± 0.40 μK
TOTAL	± 0.85 μK	± 1.13 μK

the model was verified damping factors at the FEMs were evaluated. These curves are plotted in Fig. 2.
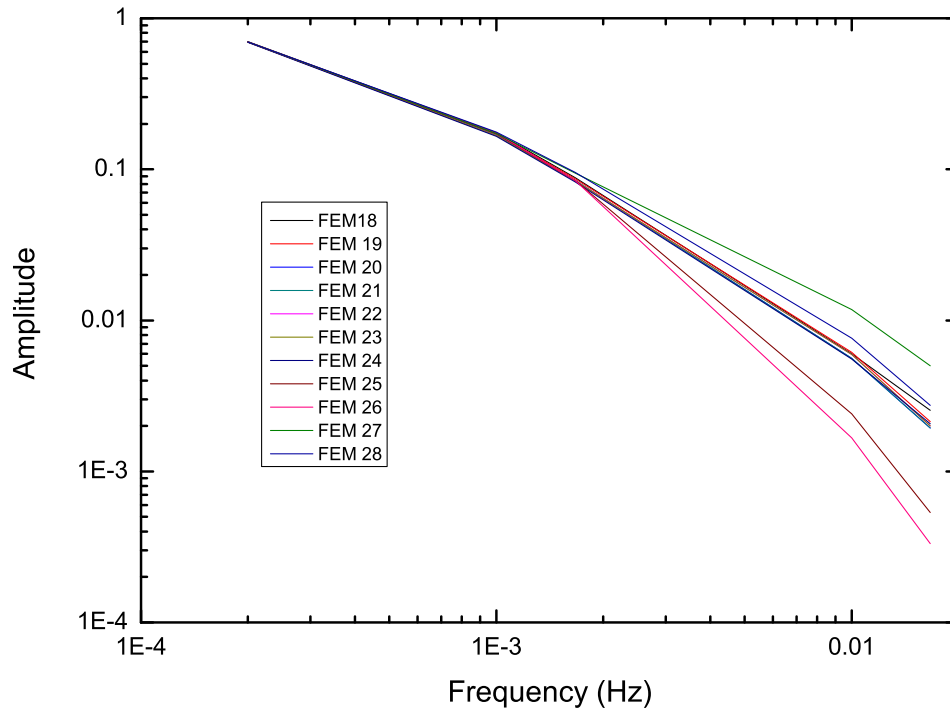

Figure 2: Thermal damping curves calculated with the ESATAN LFI thermal model.

Curves obtained from the RAA model are referred to cooler interface which is at the opposite side of the current working cooler in the first flight phase. Symmetry of the focal plane allow significance to all general considerations about final effect on maps.

4.2.1 Radiometric transfer function

The radiometric transfer function (that converts the front-end physical temperature fluctuation into the corresponding error on the sky signal measurement) can be derived from the more general radiometer equation. If we consider a variation of the physical temperature given by δT_{phys} then it is possible to calculate the corresponding variation in the measured signal following the approach described in [RD11, RD8]. This variation has the form $\delta T_{\mathrm{meas}} = T_f \times \delta T_{\mathrm{phys}}$, where T_f is the transfer function given by:

$$
\begin{aligned}
T_f &= L_{\mathrm{feed-OMT}} \left\{ (1 - L_{\mathrm{feed-OMT}}^{-1}) - r(1 - L_{4\mathrm{K}}^{-1}) + \right. \\
&\quad + \left. \left[\tilde{T}_{\mathrm{sky}} + T_{\mathrm{n_{FE}}} - r(\tilde{T}_{4\mathrm{K}} + T_{\mathrm{n_{FE}}}) \right] \frac{\log(10)}{10} \frac{\partial G_{\mathrm{dB}}}{\partial T_{\mathrm{phys}}} + (1 - r)\frac{\partial T_{\mathrm{n_{FE}}}}{\partial T_{\mathrm{phys}}} \right\}
\end{aligned}
\tag{1}
$$

In the equation above the different terms relative to the various dependencies on the physical temperature can be easily recognised. In particular we see that the transfer function depends on level of signal unbalance at the level of the first hybrid input (i.e. $\delta = \tilde{T}_{\mathrm{sky}} - \tilde{T}_{4\mathrm{K}}$), on the thermal stability of front end gain (term $\partial G_{\mathrm{dB}}/\partial T_{\mathrm{phys}}$) and noise temperature (term $T'_{\mathrm{n_{FE}}} = \partial T_{\mathrm{n_{FE}}}/\partial T_{\mathrm{phys}}$) and on the gain modulation factor, r; in particular:

- the signal unbalance δ is determined mainly by the insertion losses of the Feed-OMT system and of the 4K reference horn. In general the insertion losses of the various radiometer components (feed, OMT, hybrids, phase switches) depend on the physical temperature, but this dependence is weak for temperature changes of the order of 10 - 20 mK, and can therefore safely be neglected. Considering reference load signal of the order of 4.6K and front-end passive components with insertion losses in the range reported in table below we can expect δ to be fixed at a value in the range -1.3K to -1.8K;

- dedicated thermal susceptibilty tests allowed to estimate the values of $T'_{\mathrm{n_{FE}}}$ ranges from about 0.1 to 0.8 K/K;

- gain sensitivity to physical temperature oscillations was estimated in the same tests to be order of -0.01 to -0.2 dB/K;

- the gain modulation factor during the ground tests were depending from sky and reference load temperatures; applying the typical flight modulation factors to this analytic expression, together with other paramters estimated in the test, it is possible to predict the effect in flight, which, as reported in the Table, is anyway not far from the measurements.

    In Tab. 4 we show values of T_f obtained from measurements during LFI RCA tests.

Note that the transfer function depends both of the signal offset before the first hybrid and on the offset at the level of the front-end amplifiers. The signal offset before the first hybrid depends on the insertion loss of the front-end passive components (feed-OMT assembly and 4K reference load antenna). Of course one could in principle balance the insertion losses of the two branches in such a way to minimise the offset at this level. The reduction in susceptibility to temperature fluctuations, however, would be very small, as shown in the table above (last row).

	30 GHz	**44 GHz**	**70 GHz**
$L_{\mathrm{feed-OMT}}$ (dB)	0.1	0.1	0.25
L_{4K} (dB)	0.1	0.1	0.16
T_{phys} (K)	20	20	20
T_n (front-end, K)	10.8	14.2	29.8
$\partial G^{\mathrm{dB}}/\partial T_{\mathrm{phys}}$ (dB/K)	-0.07	-0.04	-0.07
$\partial T_n/\partial T_{\mathrm{phys}}$ (K/K)	0.36	0.36	0.25
T_f	**0.062**	**0.046**	**0.030**
T_f with no front end offset	**0.055**	**0.041**	**0.027**
T_f extrapolation to flight	**0.046**	**0.037**	**0.032**

Table 4: Values of the radiometer transfer function for front end temperature fluctuations, measured in the RCA dedicated tests. In the table we report also typical values of the LFI parameters estimated from the tests by eq. (1).

During CPV phase an estimate of the radiometer transfer function was obtained in the thermal susceptibility test (reported in [RD9]). These flight values are referred to the variation in the signal related to the variation in the temperature of the sensors located close to the detectors. In particular for the RCA28, the presence of a sensor in the flange of the horn gives a good approximation of the FEM temperature. As a preliminary sketch of the difference between a period with a stable TSA with the latest days, where fluctuations in the cooler cold end is not efficiently damped, we report here a comparative analysis of ODs 200 and 371, respectively. Data are taken from the Compact Data Set, where values are averaged each minute so that a very rough cleaning of the single scans dipole modulation is obtained. In the Fig. 3 below we show how the signal (in this case the RCA 28-00 differenced output) is very well correlated to the FPU temperature instabilities in the current fluctuating period.

Due to the consistent correlation it is possible to estimate a dynamical thermal susceptibility to compare with the CPV test result. A linear fit is obtained from the differenced output vs FH28 Flange sensor curve (see Fig. 4)

Correspnding results, reported in Table 5, confirm the scale of radiometer thermal transfer functions and provide a good approximation to estimate fluctuation effects on maps based on FH28 Flange temperature sensor curves.

Detector	28-00	28-01	28-10	28-11
T_f from CPV	0.0427	0.0290	0.0346	0.0134
T_f from OD371	0.0364	0.0224	0.0301	0.0096

Table 5: Values of the radiometer transfer function measured during CPV dedicated tests together with estimated values during OD371.

4.2.2 Analytical estimate of effect on final map

Under quite general assumptions the peak-to-peak effect of periodic oscillations in the detected signal on the reconstructed sky map can be evaluated analytically [RD6]. In fact if we consider a periodic fluctuation (δT) of general shape in the detected signal, we can expand it in Fourier

Impact of Sorption-Cooler induced temperature fluctuations on Planck-LFI: evaluation using data measured in flight.

Document no: PL-LFI-PST-TN-096
Issue/Rev. no.:   1.0
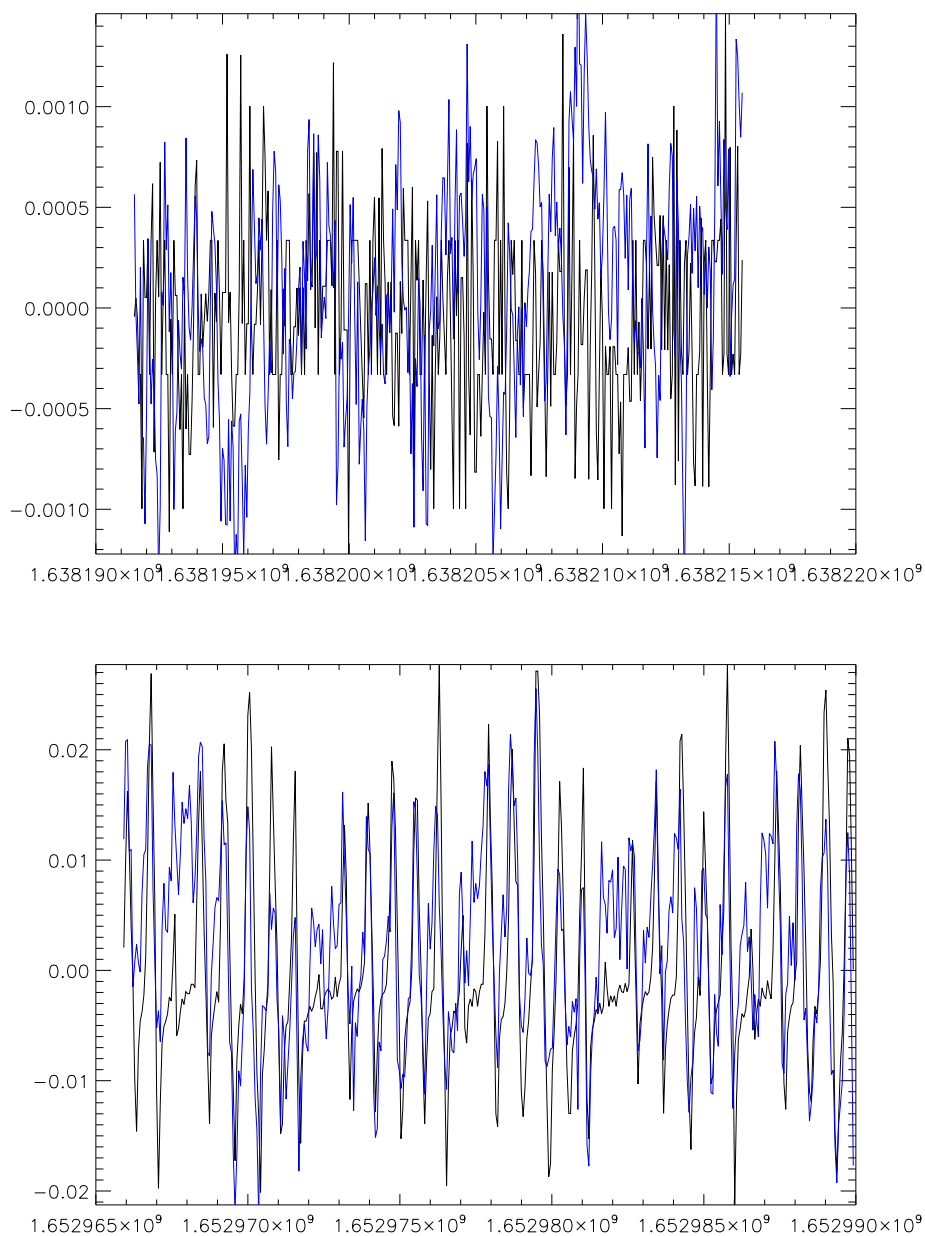Date: May 30, 2010
Page: 8 of 17

Figure 3: In the upper plot, about six hours of the feed horn 28 flange temperature sensor fluctuations (black line) are compared to RCA28-00 differenced output (blue curve, magnified 30 times) during OD200; in the lower plot feed horn 28 flange temperature sensor fluctuations (black line) are compared to RCA28-00 differenced output (blue curve, magnified 300 times) during OD371.
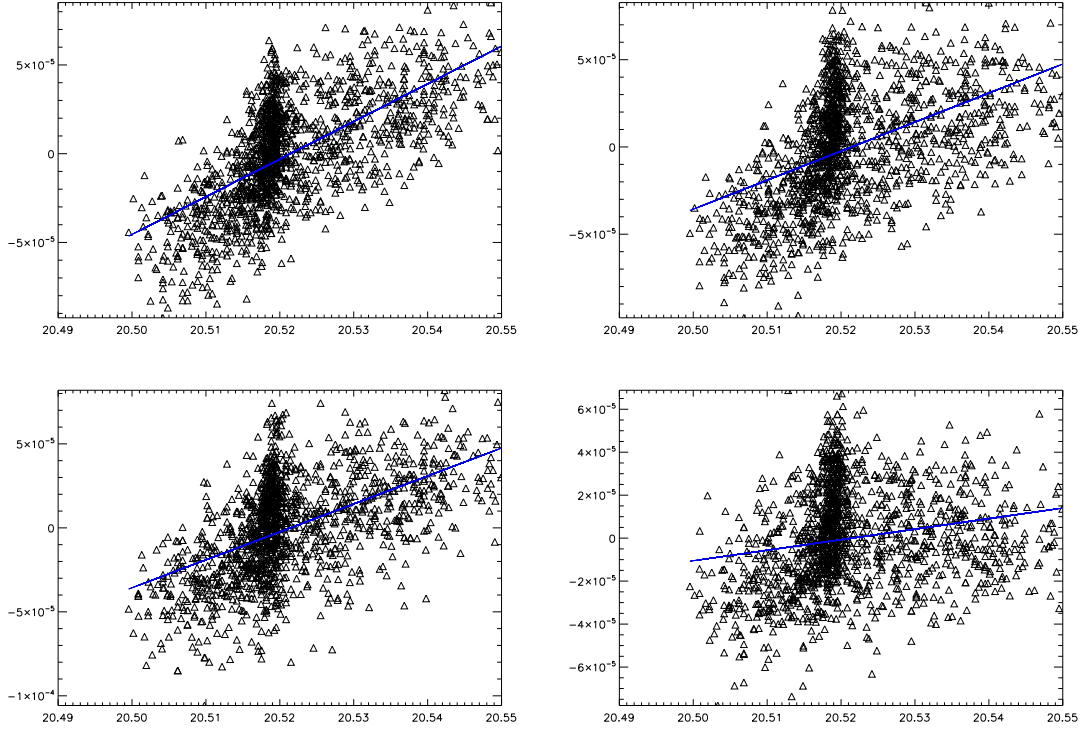
Figure 4: Measurements of the linear correlation (fit line is in blue) between FH28 Flange temperature fluctuations and RCA28 detectors differenced outputs (00 top left, 01 top right, 10 bottom left, 11 bottom right).

series, i.e.: $\delta T = \sum_{j=-\infty}^{+\infty} A_j \exp(i2\pi\nu_j t)$, where ν_j represents the different frequency components in the fluctuation.

Let us now estimate what is the damping factor for the various harmonics determined by the measurement strategy alone. To do this we consider two different regions of the frequency spectrum with respect to the satellite spin frequency, $\nu_{\rm spin}$:

- the **low frequency region**, i.e. $\nu_j < \nu_{\rm spin}$, and

- the **high frequency region**, i.e. $\nu_j \geq \nu_{\rm spin}$.

In the low frequency region each harmonic with amplitude A_j will be damped by the measurement redundancy and by the projection of the time ordered data onto a map with a pixel size $\theta_{\rm pix}$ by a factor proportional to $\sin(\pi\nu_j/\nu_{\rm spin})$. In the high frequency region, instead, we make a distinction between frequencies that are synchronous with the spin (i.e. $\nu_j = k\,\nu_{\rm spin}$) and frequencies that are not (i.e. $\nu_j \neq k\,\nu_{\rm spin}$). For the first ones there will be no damping effects as these signals are practically indistinguishable from the sky measurement, while the second will be damped by a factor of the order of $N \times \theta_{\rm pix}/\theta_{\rm rep}$ where $\theta_{\rm rep}$ represents the satellite repointing angle (i.e. the angle between two consecutive scan circles in the sky).

Tho the damping provided by the measurement redundancy we can also add an additional reduction provided by the application of destriping/map-making algorithms to the time ordered

data: if we denote with F_j this additional damping then we can write the following expression of the final peak-to-peak effect of a generic signal fluctuation δT on the map:

$$\langle \delta T^{\mathrm{p-p}} \rangle_{\mathrm{map}} \sim 2 \left[\frac{1}{N \times \theta_{\mathrm{pix}}/\theta_{\mathrm{rep}}} \left(\sum_{\nu_{\mathrm{spin}} \leq \nu_j < k\,\nu_{\mathrm{spin}}} \left| \frac{A_j/F_j}{\sin(\pi \nu_j/\nu_{\mathrm{spin}})} \right| + \sum_{\nu_j < \nu_{\mathrm{spin}}, \nu_j \neq \nu_{\mathrm{spin}}} |A_j/F_j| \right) + \sum_{\nu_j = k\,\nu_{\mathrm{spin}}} A_j \right] \quad (2)$$

where N is the number of times each sky pixel is sampled during each scan circle.

4.2.3 Systematic effects on maps from housekeeping temperature sensors

Impact of focal plane temperature fluctuations on maps can be evaluated by producing a map of a focal plane temperature sensor using pointing and sampling rate of a scientific channel.

The most suitable sensor for performing such analysis is FH28_FLANGE, which is located right on the support of the feed horn of RCA 28 and is sampled at 1 Hz.

The first step has been to filter the termometer stream in order to remove sensor noise; for this purpose we implemented a IIR (Infinite Impulse Response) filter based on 8th order Butterworth with a cutoff frequency of 0.1 Hz. Filtering is applied in time domain an operational day basis by concatenating the reversed signal at the sides of the array in order to damp possible edge effects. Gaps between operational days are of few microK and do not affect the analysis because the repointing manouvre is flagged out.

The second step has been to interpolate the signal from 1 Hz to 32.5 Hz, which is the sampling rate of a 30 GHz channel. Being the signal already smoothed by the filtering process this process has been a simple linear interpolation.

The third step has been the application of the scalar transfer function between thermometer and calibrated radiometric output; this transfer function has been measured during CPV during a dedicated test [RD10]. In this case we have considered the two extreme cases: the detector LFI28M-00, with a transfer function of 0.0134 K/K, and the detector LFI28S-11 with a transfer function of 0.0427 K/K.

Maps are shown only for the first case: because destriping is a linear process maps relative to the LFI28S-11 detector can be obtained by multiplying the LFI28M-00 maps by the transfer function ratio (3.1865).

The last step has been the production of an exchange format file for LFI28M-00 with the same flagging of the radiometric channel. The dataset can be used by Madam M3, the Madam version built for the M3 data interface library, to produce maps on the Planck cluster at NERSC.

Histograms showing the distribution of values on the maps have also been produced.

5 Results and discussion

5.1 Analytical estimate of sorption-cooler induced effect on maps

In this section we summarise the results of the analytica estimate of the peak-to-peak effect on the final maps using Equation (2). In particular in Table 6 we report the detailed results for all the detectors while in Fig. 5 we show the average effect at each LFI frequency for the three studied scenarios.

It is important to underline that the calculation, in this case, assumes a pixel size equal to physical beam size. In particular the values used in the calculation have been: 33' (30 GHz), 24' (44 GHz) and 14' (70 GHz).

Table 6: Peak-to-peak effect from Sorption Cooler temperature fluctuations on maps estimated with Equation (2. Values are in μK.

| TSA off					nominal TSA					TSA after 9 months			
RCA ID	M-00	M-01	S-10	S-11	RCA ID	M-00	M-01	S-10	S-11	RCA ID	M-00	M-01	S-10	S-11
LFI18	35.1	37.6	28.1	31.8	LFI18	4.0	4.3	3.2	3.7	LFI18	17.1	18.4	13.7	15.5
LFI19	37.7	3.6	48.2	44.6	LFI19	3.6	0.3	4.6	4.2	LFI19	17.6	1.7	22.5	20.8
LFI20	26.5	22.9	23.7	23.3	LFI20	2.5	2.2	2.2	2.2	LFI20	12.4	10.7	11.1	10.9
LFI21	12.1	7.2	3.1	3.7	LFI21	1.2	0.7	0.3	0.4	LFI21	5.7	3.4	1.5	1.8
LFI22	22.8	20.9	22.9	24.3	LFI22	2.2	2.0	2.2	2.4	LFI22	10.7	9.8	10.7	11.4
LFI23	8.6	17.9	16.7	15.9	LFI23	0.9	1.8	1.7	1.6	LFI23	4.1	8.6	8.0	7.6
LFI24	2.8	1.4	4.7	2.2	LFI24	0.3	0.1	0.5	0.2	LFI24	1.3	0.7	2.2	1.0
LFI25	3.4	2.9	6.5	5.0	LFI25	0.1	0.1	0.3	0.2	LFI25	1.5	1.2	2.8	2.1
LFI26	14.7	14.3	15.2	14.7	LFI26	0.5	0.4	0.5	0.5	LFI26	6.2	6.0	6.4	6.2
LFI27	3.2	2.0	6.8	5.9	LFI27	0.6	0.4	1.3	1.2	LFI27	1.8	1.1	3.8	3.3
LFI28	0.5	0.9	2.0	3.4	LFI28	0.1	0.1	0.2	0.4	LFI28	0.2	0.5	1.0	1.7
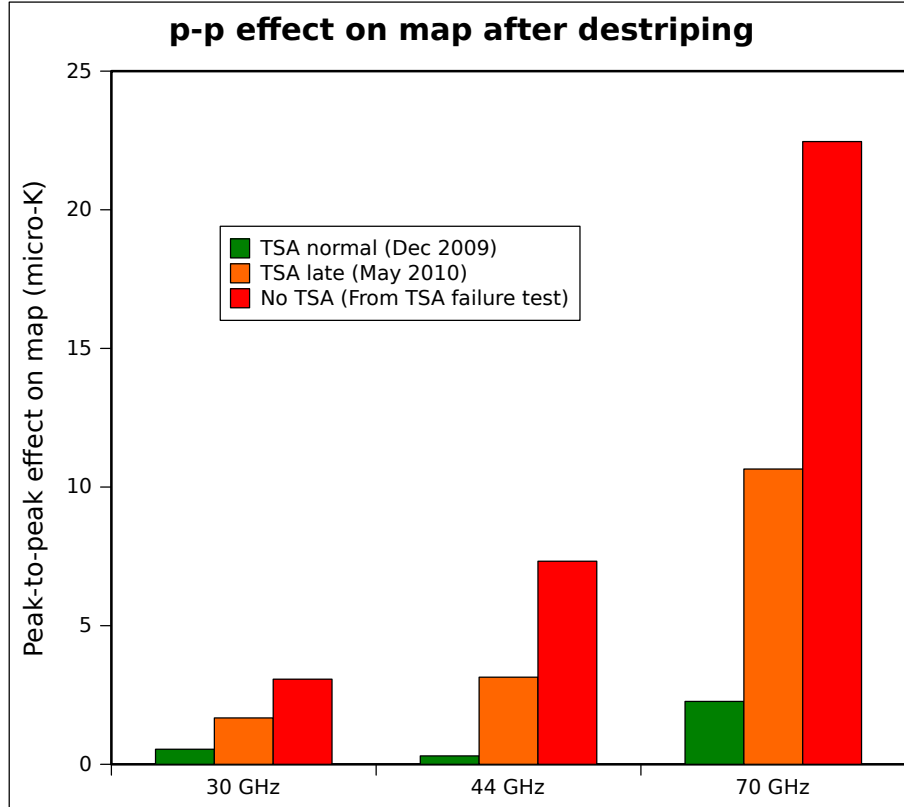
Figure 5: Estimated average peak-to-peak effect on maps at the three LFI frequencies for the studied scenarios

From the figure the beneficial effect of the TSA in nominal conditions is apparent, as expected, while the TSA in the current condition stands in between the optimal case and the worst case in which no TSA is present. In this last case, in particular, a systematic effect of several μK would be expected on maps if operated in such conditions for a time long enough to cover a significant fraction of the sky.

To verify the validity of the analytical aproach we have also performed another calculation, relative to the receiver LFI28, with results that are directly comparable with those obtained by

Impact of Sorption-Cooler induced temperature fluctuations on Planck-LFI: evaluation using data measured in flight.

Document no: PL-LFI-PST-TN-096
Issue/Rev. no.:   1.0
Date: May 30, 2010
Page: 12 of 17

the maps shown in Section 5.2. In this case we have used temperature data from the temperature sensor FH28_FLANGE (the same used to produce the maps) with the same radiometric transfer functions for the detectors `LFI28M-00` (0.0134 K/K) and `LFI28S-10` (0.0427 K/K).

Furthermore we have considered a pixel size of 6.85' corrisponding to the pixel size of maps with $N_{\mathrm{side}} = 512$ (which has been used to produce maps from housekeeping sensor data). The comparison between analytical calculations and map simulations is summarised in Table 7.

Table 7: Comparison of peak-to-peak effect from Sorption Cooler temperature fluctuations on maps estimated with Equation (2) and from direct map-making. Values are in μK. Pixel size used in the calculation has been 6.85', corresponding to the pixel size of a map with $N_{\mathrm{side}} = 512$. **Notice that the temperature fluctuation in the interval OD 262-322 (fourth column) were nominal for about the first half of the interval and slowly increasing in the second half. The analytical calculation, instead, assumes degraded fluctuations for a time span corresponding to one survey. This explains the discrepancy between the calculated and simulated effect in this case.**

	Nominal TSA		TSA after 9 months	
	Eq.2	From map OD 105-165	Eq.2	From map OD 262-322
LFI28M-00	1.78	1.33	13.10	2.00
LFI28S-11	5.79	4.24	42.67	6.37

From the comparison results we see that there is a good agreement between the analytical and direct-map estimates in the case of nominal TSA behaviour. In the case of non nominal TSA behaviour, instead, the analytical calculation over-estimates the effect with respect to the direct map making. This can be understood if we consider that in the period considered in the map-making (OD 262-322) the cooler fluctuations slowly degraded from nominal to che current fluctuation levels. The analytical calculation, instead, assumes that the fluctuation shape remains constant thoughout the survey at the current, degraded level.

This comparison once more shows the validity of the analytical approach when applied to cases in which the periodic fluctuation is stationary over long times. Therefore the results shown in Fig. 5 can be considered representative of the impact on science in various TSA scenarios assuming stationarity in the temperature fluctuations over long times.

## 5.2 Simulation of sorption-cooler induced effect on maps

In this section we shows the results of the direct map-making of temperature sensor data multiplied by the transfer function of detector `LFI28M-00` according to the procedure explained in Section 4.2.3. Maps of the effect expected for `LFI28S-11` can be estimated by multiplying the sigma and peak-to-peak by the ratio of their transfer functions (3.1865).

In Figures 6 we show maps of the thermal systematic effects without running any destriping code in the two time intervals: OD 105-165 (TSA running nominally), and OD 262-322 (temperature fluctuations slowly increasing due to cooler aging). These maps **are not** representative of the impact on science, but are useful to understand the kind of signature on the sky that has to be removed from the destriping code.

In Figure 7 we show the same maps after destriping. In this case the signature is representative of the final systematic effect. Notice that the final peak-to-peak that one derives directly from the map seems very high: this is due to a very limited number of outsiders. In oder to fully appreciate

FH28_FLANGEbest_meanremoved_filt_LFI28M-00_105-165_512_60s_binned
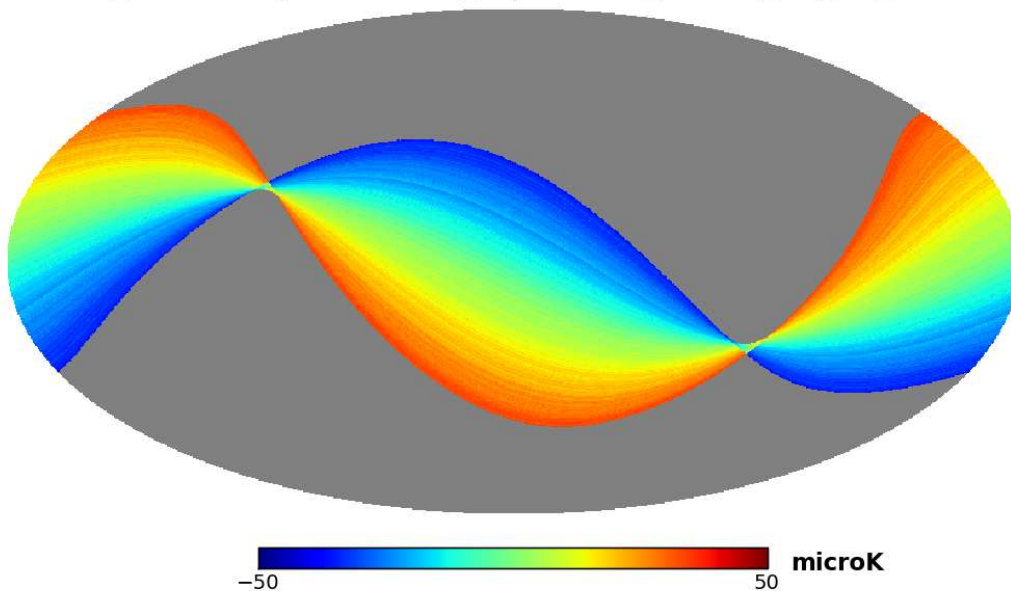
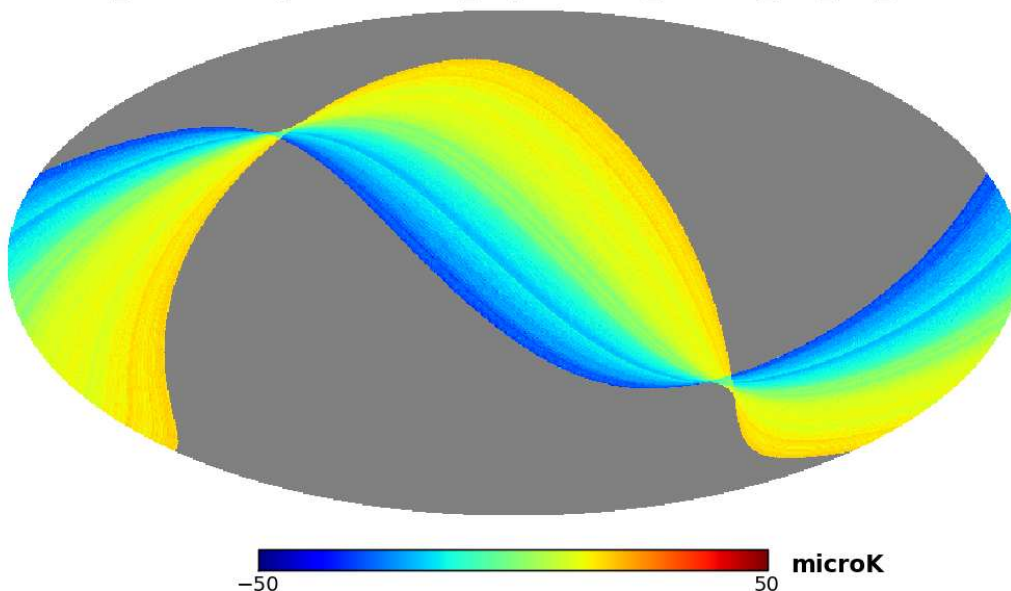FH28_FLANGEbest_meanremoved_filt_LFI28M-00_262-322_512_60s_binned

Figure 6: Binned maps 105-165 and 262-322

the distribution of the values on the map we report the histograms of the maps in Figure 8. In order to neglect outsiders we can define, from these histograms, the peak-to-peak effect in terms of the maximum difference between values in the range containing the 99% of samples. These values are

reported in the figure as well as in Table 7. The obtained results confirm the increased systematic signature caused by the increase in focal plane temperature fluctuations ($\sim 30\%$ increase in the systematic effect rms).
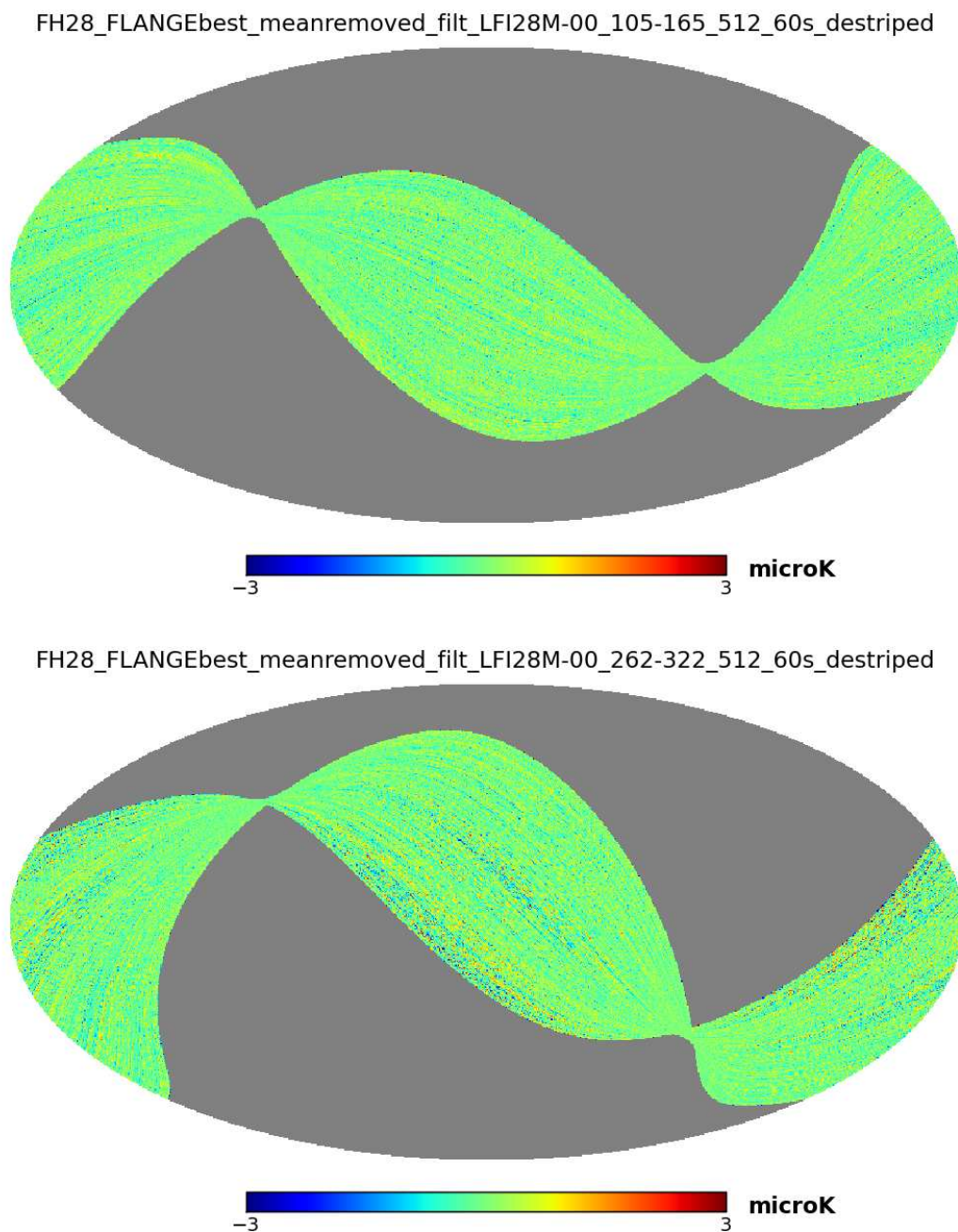
FH28_FLANGEbest_meanremoved_filt_LFI28M-00_105-165_512_60s_destriped

FH28_FLANGEbest_meanremoved_filt_LFI28M-00_262-322_512_60s_destriped

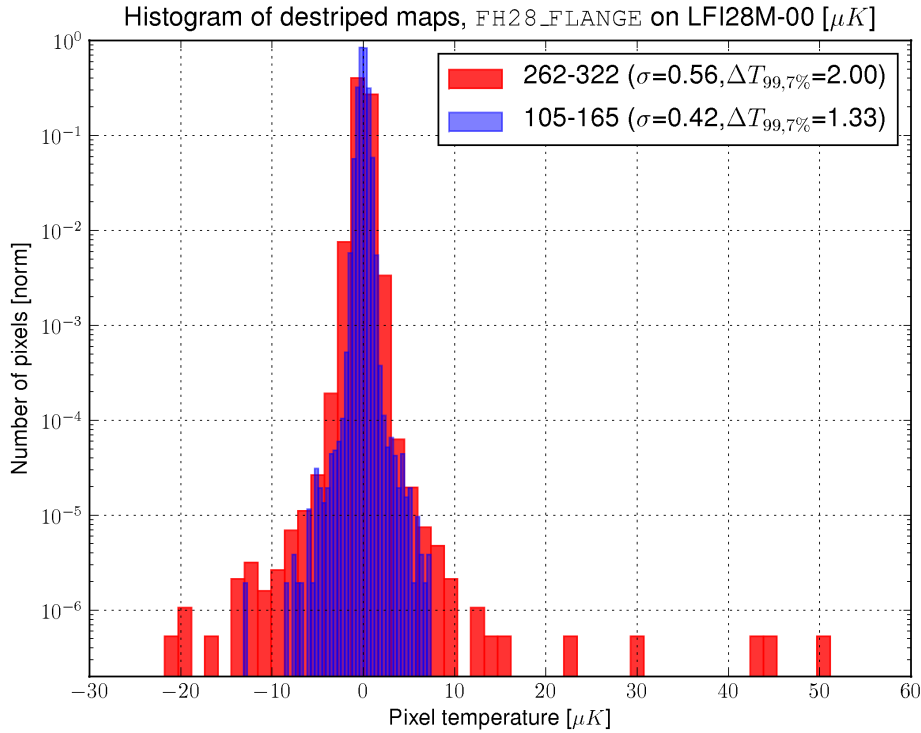**Figure 7:** Destriped maps 105-165 and 262-322

Figure 8: Histogram comparing maps 105-165 vs 262-322, σ is the standard deviation of the map, 99.7 percent of the map pixels stays within $\pm\Delta T_{99,7\%}$, both in μK

Finally we have calculated the thermal systematic effect signature for `LFI28M-00` using data from all first sky survey (OD 92-275). During this time span the temperature fluctuation level has been relatively stable at the nominal level.

The results are shown in Figures 9 (map) and 10 (histogram) and similar to those shown in Figures 7 and 8, which are relative to a shorter time span. It is worth noting that the standard deviation of the first survey map is slightly lower than the 105-165 map presumably because to double coverage of some parts of the sky.

6 Conclusions

In this technical note we have reported the results of an assessment study of the impact of focal plane temperature fluctuations on LFI maps. The study has considered three scenarios: (i) TSA is completely off and the LFI is subject to the complete spectrum of the cold end temperature variations; (ii) TSA is working nominally and, (iii) the TSA is working in a not-nominal situation because of sorption-cooler aging.

The analysis has been peformed using two independent methods to evaluate the impact on maps: the first method relies on analytical calculations of the peak-to-peak effect on the final maps according to [RD6], while the second uses direct map-making of temperature sensor data filtered by thermal and radiometric transfer functions. In this second case the used temperature

Impact of Sorption-Cooler induced temperature fluctuations on Planck-LFI: evaluation using data measured in flight.

Document no: PL-LFI-PST-TN-096
Issue/Rev. no.:   1.0
Date: May 30, 2010
Page: 16 of 17

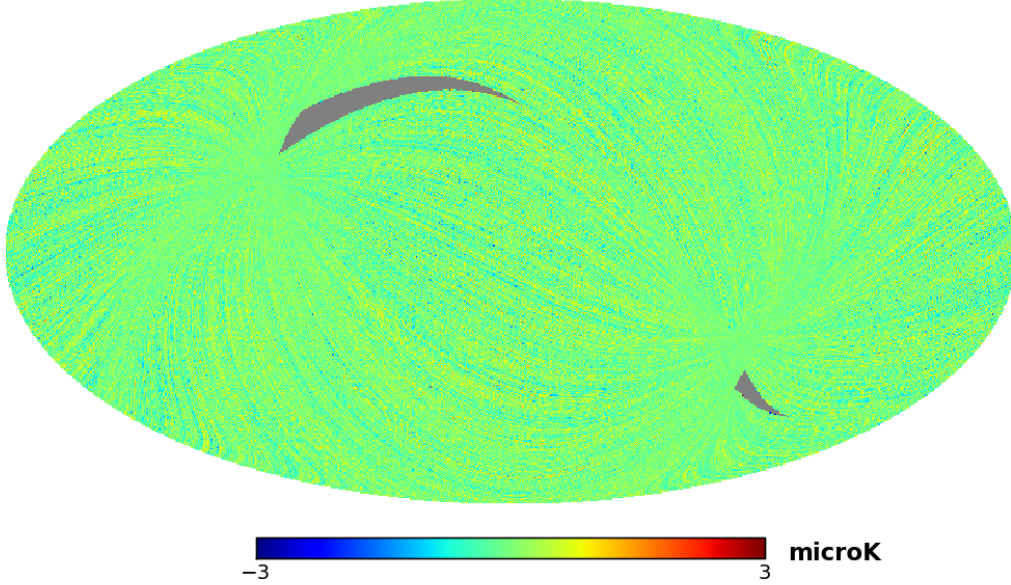FH28_FLANGEbest_meanremoved_filt_LFI28M-00_92-275_512_60s_destriped

Figure 9: Destriped map of the first survey

sensor (`FH28_FLANGE`, placed directly on the LFI28 feed horn flange) allowed to neglect the thermal transfer function so that only the radiometric part was used.

The comparison between the two methods (oulined in Table 7) confirms the validity of the analytical estimate in cases where the temperature fluctuation can be considered stationary over long times (a significant fraction of a survey).

The evaluation of the impact on science of the three scenarios (reported in Figure 5 and in Table 6) shows that if temperature fluctuations are stabilised by the TSA at the nominal level then the expected effect on maps is small and compatible with LFI scientific requirements reported in [AD1] and summarised in Table 3. This confirms the correctness of the LFI focal plane unit thermal stability design and the need of the TSA at the interface between the Sorption cooler cold end and the instrument.

With the level of temperature fluctuations measured in the last month (from late April through May 2010) the effect clearly increases and becomes only marginally compatible with the LFI requirements should the fluctuations continue at this level for a significant fraction of the second-survey sky coverage.

Finally, if whe TSA were shut off then the impact on LFI maps would be of several μK and not compatible with LFI scientific requirements. This would be especially true for the 70 GHz channels, which are characterized by a smaller pixel size and would be affected by residual systematic uncertainties of more than 10 μK. This level of residual effect would impact, in particular, the imaging capabilities of the instrument and the corresponding scientific analysis relying on accurate CMB maps, like, for example, non gaussianity studies.
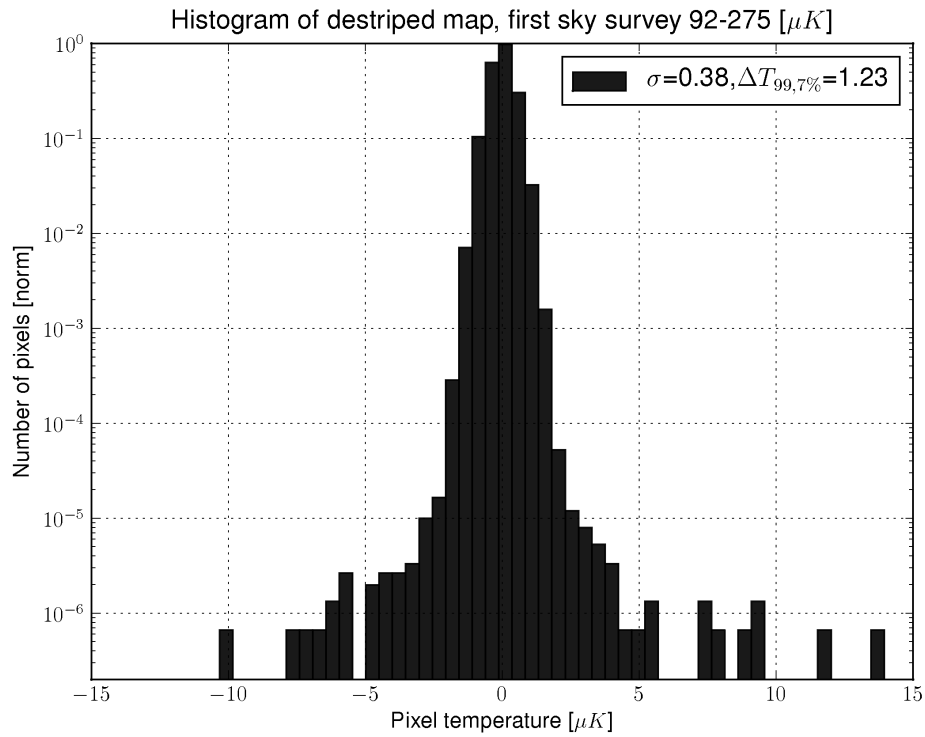
Impact of Sorption-Cooler induced temperature fluctuations on Planck-LFI: evaluation using data measured in flight.

Document no: PL-LFI-PST-TN-096
Issue/Rev. no.:   1.0
Date: May 30, 2010
Page: 17 of 17

Figure 10: Histogram of `FH28_FLANGE` map for the first survey, σ is the standard deviation of the map, 99.7 percent of the map pixels stays within $\pm\Delta T_{99,7\%}$, both in μK